ORGANIZED STRUCTURES IN DEVELOPING TURBULENT FLOW WITHIN AND ABOVE A PLANT CANOPY, USING A LARGE EDDY SIMULATION

MANABU KANDA

Department of Civil Environmental Engineering, Yamanashi University, Kofu 400, Japan

and

MIKIO HINO

Faculty of Policy Studies, Chyu-o University, Hachi-o-ji 192-03, Japan

(Received in final form 5 August, 1993)

Abstract. A Large Eddy Simulation (LES) model representing the air flow within and above a plant canopy layer has been completed. Using this model, the organized structures of turbulent flow in the early developmental stages of a crop are simulated and discussed in detail.

The effect of the drag due to vegetation is expressed by a term added to the three-dimensional Navier–Stokes equation averaged over the grid scale. For the formulation of sub-grid turbulence processes, the equations for the time-dependent SGS (Sub-Grid-Scale) turbulence energy equation is used, which includes the effects of dissipation (both by viscosity and leaf drag), shear production and diffusion.

The organized structure of turbulent flow at the air-plant interface, obtained numerically by the model, yields its contribution to momentum transfer. The three-dimensional large eddy structures, which are composed of spanwise vortices ('rolls') and streamwise vortices ('ribs'), are simulated near the air-plant interface. They are induced by the shear instability at inflection points of the velocity profile. The structure clearly has a life cycle. The instantaneous image of the structure is similar to those observed in the field observations of Gao *et al.* (1989) and in the laboratory flume experiments of Ikeda and Ota (1992). These organized structures also account for the well known fact that the sweep motion of turbulence dominates momentum transport within and just above a plant canopy, and the motion of ejection prevails in the higher regions.

1. Introduction

Much effort has been expended to advance understanding of the mechanism of momentum transfer between the atmosphere and a plant canopy. Since the 1960's, gradient-type diffusion theories on flow over a plant canopy have been developed by many researchers (e.g., Inoue, 1955; Kondo and Akashi, 1976). These theories have contributed greatly to understanding of mean-wind velocity profiles within and above a plant canopy. In the latter half of the 1970's, high-order closure models were applied to the turbulent flow within and above a plant canopy (e.g., Wilson and Shaw, 1977; Inoue, 1981; Yamada, 1982). These models accounted for not only the mean velocity profiles but also the statistical features of turbulence much better than did the gradient diffusion theory.

In recent years, the contributions of coherent structures of turbulent flow, such as sweeps and ejections, to momentum transfer have been vigorously studied by

Boundary-Layer Meteorology **68**: 237–257, 1994.

quadrant analysis or probability analysis based on field measurements (Finnigan, 1979; Shaw *et al.*, 1983; Shaw and Seginer, 1987; Maitani and Shaw, 1990). These studies showed that, within and just above a plant canopy, sweeps are more efficient than ejections for the transfer of momentum. However, the spatial or temporal images of organized structures have not been studied in detail because of measurement difficulties. Gao *et al.* (1989) using seven sonic anemometers obtained ensemble-averages of the organized structure within and above a forest canopy, which corresponds to the ramp pattern of temperature variation. The eddy structure indicated by them is large; it extends down to a level near the ground and up to about twice the height of the plant canopy. The result is quite different from the organized structure, i.e., horseshoe eddy or pair-vortex as observed in the wall region or the low atmosphere. Bergstorm and Högstrom (1989) investigated the organized structure above a pine forest and showed that ramp-events constituted a large part of the total fluxes of momentum. These results suggest the importance and the need for an understanding of the organized structure itself. It is difficult to measure the instantaneous spatial motion and to obtain a three-dimensional image of turbulence structure near the canopy surface in the field or laboratory, but numerical methods can provide much spatial and temporal information about these organized structures. The Large Eddy Simulation method, which was developed by Deardorff (1970) and applied to turbulent flow between two parallel plates, is one of the most powerful means to investigate, (a) the instantaneous turbulent motion of air flow within and above the plant canopy; and (b) their effects on momentum transfer between air flow and plant canopy. This method allows one to calculate temporal fluctuations directly even though they are grid-averaged. Most recently, Shaw and Schumann (1992) performed an LES of turbulent flow above and within a forest. They presented a picture of an instantaneous vertical velocity field at a fully-developed turbulent stage. The purpose of this paper, as noted below, is rather to investigate the large eddy structures of turbulence and their temporal development in detail.

Another difficulty is caused by 'plant waving' , that appears to be closely related to the organized structure within and above a plant canopy. Two kinds of mechanisms have been proposed for plant waving. One is the resonance between the air flow above the canopy and the waving of the plants. The turbulence in the velocity and pressure of the air flow have the same frequency as does the plant vibration. The other is the so-called 'Honami', which is the wave-like travelling disturbance in grassy canopies caused by a travelling gust (Inoue, 1955). The mechanism, which is supported by experimental evidence, is that the oscillation peaks in spectra and cospectra of u' and w' correspond to the frequency of gusts. A large turbulent eddy is advected with the velocity of the mean flow and forces the plant to oscillate. Even if the plant canopy were composed of nonelastic materials, wave-like fluctuations within plant canopies could occur in accordance with the latter mechanism. Though such 'sweep and ejection cycles' and 'wave-like fluctuations' are typical features of turbulence within and above plant can-

opies, they are analysed in a similar way and display the same images as do 'near wall turbulence' flows (for example, the quadrant analysis mentioned above). However, the velocity profile within and above the plant canopy has its inflection point near the canopy top. This fact suggests an analogy of canopy flow to the flow in the mixed layer rather than to that in the wall regions (Raupach *et al.*, 1989; Raupach *et al.*, 1991). Ikeda *et al.* (1992) pointed out, by use of both a linearized theory and laboratory experiments, that the shear instability at an inflection point of the velocity profile near an air-plant interface gives rise to wave-like fluctuations of momentum.

Our parameterization of turbulence within plant canopies is quite idealized because it does not include details about real plants like the shape of each leaf, branch and stem, and the consequences of waving. The purpose of the present work is rather to simulate the turbulent coherent structure within and above a plant canopy that is induced by shear-instability and to examine whether and to what degree these structures can explain the turbulent characteristics within a plant canopy presented in the previous studies. In this paper, the developing rather than the fully-developed stage of turbulence is discussed. One reason for this is that temporal changes of turbulent structures are more clearly seen and more easily discussed in the developing stages of a turbulent mixing shear layer. Another reason is that the computational domain size adopted in this paper is unfortunately not large enough to discuss the fully-developed stage of turbulence because of computational costs.

2. Development of a Numerical Model of the Plant Canopy Layer Using the LES Method

The structure of real plants is so complicated that one cannot readily express data for each leaf and stem of a plant in a finite-difference grid. Therefore a numerical model was constructed based on a virtual element that works more for the whole plant canopy. The model and results to be described is an extension of the paper by Hino *et al.* (1992) and Kanda *et al.* (1992a, b).

The following assumptions and simplifications were made in the model:

(1) The space occupied by leaves was neglected. The thickness of a leaf is about 1 mm and the leaf area density is 5.0 (m^2/m^3); thus the volume occupied by leaves is only 0.5% – a volume that can be neglected.
(2) The distribution of the leaves was represented only by the leaf area density. (The shapes of leaves and stems were not taken into consideration.)
(3) The waving motion of plant was neglected.

a. Governing equations

Air flow within and outside a plant canopy can be described by the law of

momentum conservation, i.e. by the Navier–Stokes equations with additional terms for the drag of plant leaves,

$$\frac{Du_i}{Dt} = -\frac{1}{\rho}\frac{\partial p}{\partial x} + \frac{\partial R_{i,j}}{\partial x_j} - C_m S U^2 \frac{u_i}{|U|}. \tag{1}$$

Here $i, j = 1, 2, 3$ correspond to x, y, z, respectively; x is in the downstream direction, y is in the spanwise direction and z is upward. The quantities $u_1(=u)$, $u_2(=v)$ and u_3 $(=w)$ are the grid-averaged velocity components in each direction, p is the mass density of air, U is the magnitude of the total velocity vector $(\sqrt{u_i u_i})$, p is the grid-averaged pressure, g is the gravitational acceleration, C_m is the drag coefficient, S is the leaf area density, t is time and R_{ij} represents the SGS (Sub Grid Scale) Reynolds stress term (defined in Equation (4)). The continuity equation is given by

$$\frac{\partial u_i}{\partial x_i} = 0. \tag{2}$$

The MAC (Marker-And-Cell) method of numerical computation of fluid flow (Harlow and Welch, 1965) was used in solving for the pressure field. It yielded a Poisson-type equation for p from Equations (1) and (2),

$$\nabla^2 p = \frac{\partial}{\partial x_i}\rho\left[-u_j\frac{\partial u_i}{\partial x_j} + \frac{\partial R_{i,j}}{\partial x_j} - C_m S U^2 \frac{u_i}{|U|}\right] - \frac{\theta}{\partial t}\left[\frac{\partial u_i}{\partial x_i}\right], \tag{3}$$

where the last term in the right hand side represents the correction term for the mass conservation introduced in the MAC method. To maintain the flow against the drag forces by the canopy and the walls, the pressure gradient in the x direction is modified at each time step of numerical integration so as to keep the mass flux at a constant value.

b. The SGS turbulence model

The SGS Reynolds stress terms $R_{i,j}$ in Equation (1) are as follows (Smagorinsky, 1963):

$$R_{i,j} = K_m\left[\frac{\partial u_i}{\partial x_j} + \frac{\partial u_j}{\partial x_i}\right] - \frac{2}{3}\delta_{i,j}E, \tag{4}$$

where K_m is the SGS eddy mixing coefficient, $E = (u_i' u_i'/2)$ is the SGS kinetic energy and a prime $(')$ indicates the deviation from the grid-averaged values. Once E is known, K_m can be determined from the following equations, first derived by Schumann (1975),

$$K_m = C_1 E^{1/2} L, \tag{5}$$

where L is the appropriate sub-grid length scale $L = (\Delta x\, \Delta y\, \Delta z)^{1/3}$ (where Δx,

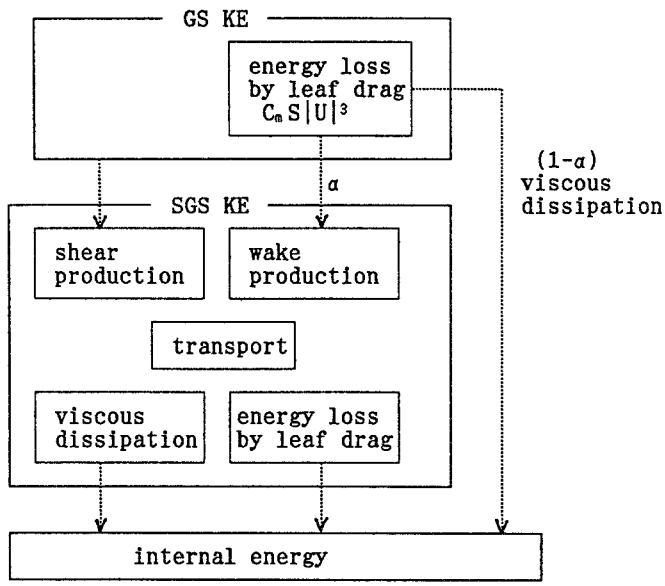

Fig.1. A schematic of the kinetic energy transformation pathways included in the model.

$\Delta y, \Delta z$ are grid intervals in the x, y, z directions, respectively), and C_1 is a parametric constant.

The equation for SGS kinetic energy E can be written as follows:

$$\frac{DE}{Dt} = R_{i,j}\frac{\partial u_i}{\partial x_j} + \frac{\partial}{\partial x_j}\left[K_m \frac{\partial E}{\partial x_j}\right] - \frac{C_2}{L}E^{3/2}$$
$$- C_m S(2E)|U| + \alpha C_m S|U|^3. \tag{6}$$

Here the terms on the right hand side of Equation (6) represent successively the effect of SGS shear production, SGS diffusion, SGS dissipation by viscosity, SGS energy loss by the drag force due to leaves, and SGS wake production by the drag of the leaves. The quantity α is the ratio of the transformation of energy loss in grid-scale flow by leaf drag to wake production in SGS flow. The value of α can vary from 0.0 to 1.0. Figure 1 is a schematic of the kinetic energy transformation pathways included in the model. The SGS turbulence energy loss due to the drag of the leaves was assumed to be directly transformed to internal energy ($-C_m S(2E)|U|$). This assumption is acceptable in SGS flow, but not in GS flow, because small-scale motions dissipate quickly. In contrast, grid scale energy loss due to leaf drag ($C_m S|U|^3$) transforms into both wake production in SGS ($\alpha C_m S|U|$) and internal energy ($(1-\alpha)C_m S|U|^3$) by direct dissipation. For $\alpha = 1.0$, the energy loss in grid-scale flow by drag is completely transformed to wake production in SGS flow. Though the sensitivity of the solution to α seems to be a very important problem, it is beyond our present purpose and should be investigated separately

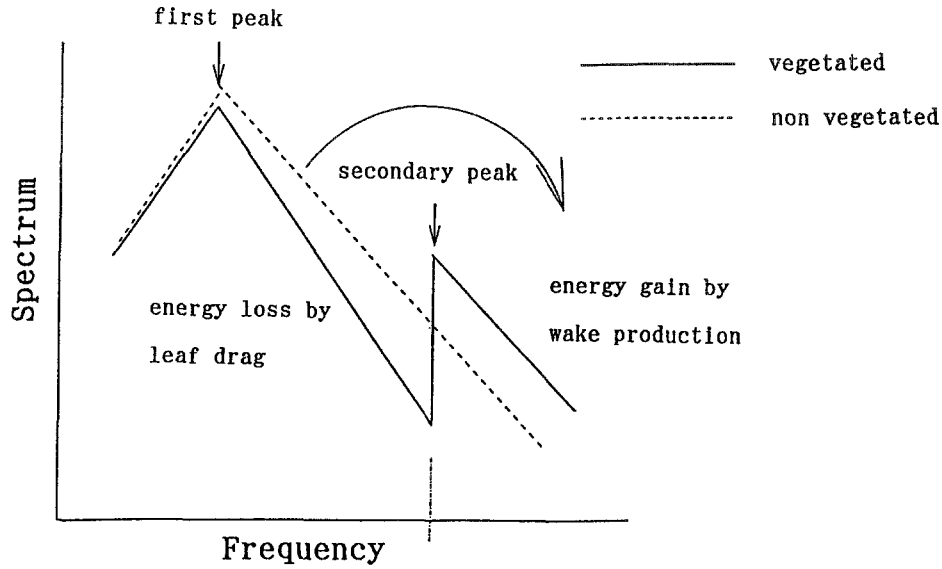

Fig. 2. An idealized schematic of the typical power spectrum of turbulence within plant canopies for a nearly neutral condition.

(Kanda *et al.*, 1992b). In this paper, the virtual leaf elements were assumed to be much smaller than the grid size, so that α was assumed to be relatively small, 0.1. The formulation of Equation (6), except for the last two terms, is similar to that used by Schumann (1975) and others. In accordance with Yoshizawa and Horiuchi (1985), constant values were assumed for the two parameters, $C_1 = 0.05$, $C_2 = 1.0$.

c. Discussion on the effects of plants

Figure 2 shows an idealized schematic of a typical power spectrum of turbulence within a plant canopy for a nearly neutral condition. In comparison with results observed for surface layers, the spectrum within a plant canopy has the following features (see for example, Baldocchi *et al.*, (1988), and Amiro and Davis (1988)): the spectral slope at low frequencies region I) is steeper than $-2/3$, and that at high frequencies (region II) is about $-2/3$; as a result, a secondary peak exists between the two regions. For low frequencies (I), large eddies cascade down to small eddies as a result of both nonlinear effects and the leaf drag. At high frequencies (II), dominant eddies are smaller than leaf elements, and they cascade down to small eddies because of nonlinear effects. These steep spectral slopes indicate a high rate of energy loss, which results from work done by both the mean kinetic energy and the shear-produced kinetic energy against the leaf drag. These effects are accounted for by the last term in Equation (1), which represents a sink of both momentum and GS turbulence energy.

Whether small eddies produced by each leaf should be included in a sink term

or a source term in Equation (6) depends on the size of the grid scale relative to that of a leaf. If the grid scale is smaller than that of eddies produced by a leaf (I), so that small eddies can be calculated directly, the source term for the drag is not used. If the grid scale is greater than the eddy size (II), the effect of leaves on SGS turbulent kinetic energy should be treated both as a sink and a source in Equation (6), as mentioned above.

3. Method of Computation

a. Finite difference method

Except for the advection terms, which are discretized by the fourth-order upwind difference (Kawamura and Kuwahara, 1984), the second-order center difference method was applied to perform the computation with a high degree of accuracy and to fulfil the stability condition. The temporal differences were approximated by a first-order implicit scheme of the Euler type. The time step was set at $\Delta t = 0.048$ s.

b. Computational domain

The height of the plant canopy, which has a uniform leaf area density, was set at 0.33 m, and the total height of the computational domain was selected to be 1 m, or about three times canopy height. The horizontal length of the model was 1.5 m in the x-direction and 1 m in the y direction, as determined from a linear stability analysis of shear flow (Ho and Huerre, 1984, with reference to Equation (7)). The number of grid points is $32 \times 20 \times 30$ in the x, y and z directions, respectively. The mesh spacing is taken to be uniform in the x and y directions, but non-uniform in the z direction, with finer resolutions near the walls and canopy top; mesh intervals vary in a geometric ratio with the ratio 1.1 in the z direction.

c. Initial and boundary conditions and parametric values

At the upper and lower boundaries, a non-slip condition was used. We decided not to use an open boundary condition because it has not been adequately investigated with a LES; in fact, a preliminary run using an open boundary condition gave unsatisfactory results.

At the lateral boundaries, cyclic conditions were chosen because the turbulence eddies near the air-plant interface can be advected over the whole region by the mean flow before enough time has elapsed for complete flow development in the restricted domain. Ho and Huerre (1984) performed a linear stability analysis on a mixing shear layer, consisting of two layered laminar streams that have different mean velocities, to obtain the relationship between the amplification rate of a disturbance and the Strouhal number. According to them, the Strouhal number of an infinitesimally stable disturbance which has maximum amplification rate is given by

TABLE I

Relevant information concerning the cases investigated

Mass flux	Q	$= 0.40$ (m^3/s)
Leaf area density	S	$= 2.5$ (m^2/m^3)
Drag coefficient	C_m	$= 0.5$
LES constants	C_1	$= 0.05$
	C_2	$= 1.0$

$$S_t = f\sigma/U_{1+2} = 0.032\,, \tag{7}$$

where S_t is Strouhal number, f is frequency of the disturbance, σ is initial momentum thickness of the shear layer, and U_{1+2} is the average of the velocities of the two parallel streams. Using the initial velocity distribution, we can determine f and a wavelength. The length of the computational domain in the x direction was chosen to be twice as large as the theoretical wavelength calculated from Equation (7). Because of this restriction of domain size, only the developing stages of a turbulent flow can be discussed in this paper.

The initial velocity distributions were determined as follows. First, Equations (1) and (3) were solved using only u and p (that is, with v and $w = 0$) in such a way that mass flux in the x direction is kept constant, and then the mean-velocity profile of u was determined. Random noise was then superimposed on each velocity component with a maximum amplitude of 1% of the mean velocity. Table I gives relevant information concerning the cases investigated.

4. Results and Discussion

a. Cyclic development of organized structure – wave-like fluctuations

Figures 3 and 4 represent the temporal change of spanwise and streamwise vortices (η, ξ) in the xz plane ($y = 0$). A layer (Figure 3a) with high-intensity vorticity is generated near the top of the plant canopy. Two large spanwise vortices (Figure 3b) then develop as time passes; i.e., in the initial stage, the structure of the turbulent field is two-dimensional in the spanwise direction. At $t = 14.3$ s, streamwise vortices appear (Figure 4b), even though no prior streamwise vortex existed initially. Such large-scale spanwise vortical structures (rolls) were first found by Brown and Roshko (1974) in a plane mixing layer, and the existence of streamwise vortices was confirmed by Bernal and Roshko (1986). At $t = 16.7$ s, the two large eddies merge, and then they grow to form a bigger vortex (Figure 3c, d) whose wavelength is twice as large. As the spanwise vortex grows, the streamwise vortices intensify, and they can be clearly identified (Figure 4c, d). Figure 5 shows the seven stages of the evolution of streamwise vortices (ξ) in a yz cross-section (the

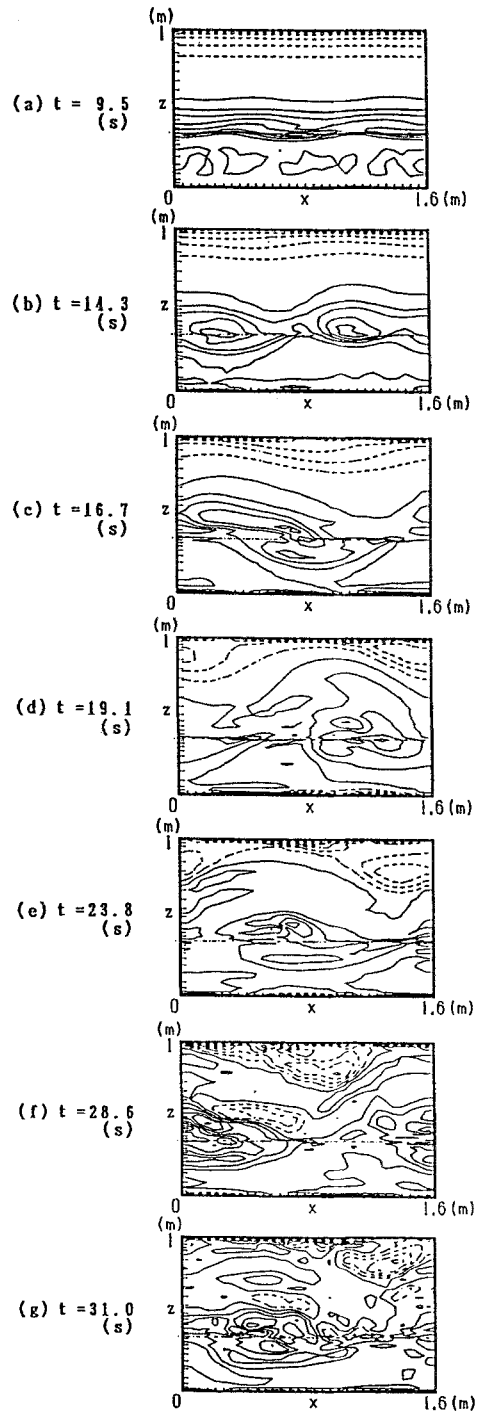

Fig. 3. Spanwise vortices (η) in the xz cross-section ($y = 0$) at seven time stages; (a) 9.5 s, (b) 14.3 s, (c) 16.7 s, (d) 19.1 s, (e) 23.8 s, (f) 28.5 s, (g) 31.0 s. Contour interval is 1.0 s^{-1}. Dotted line indicates a negative value.

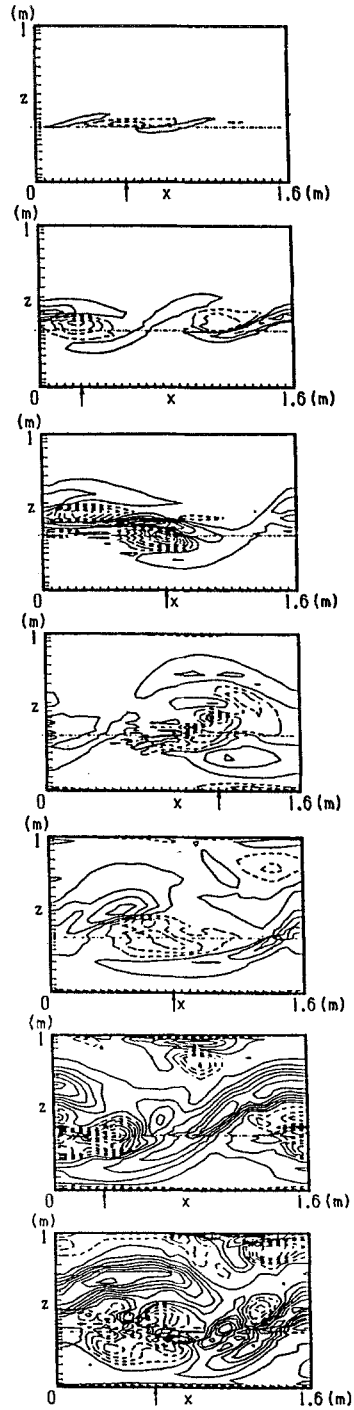

Fig. 4. Streamwise vortices (ξ) in the xz cross-section ($y = 0$) at seven time stages, same as in Fig. 3. Contour interval is $0.5\,s^{-1}$.

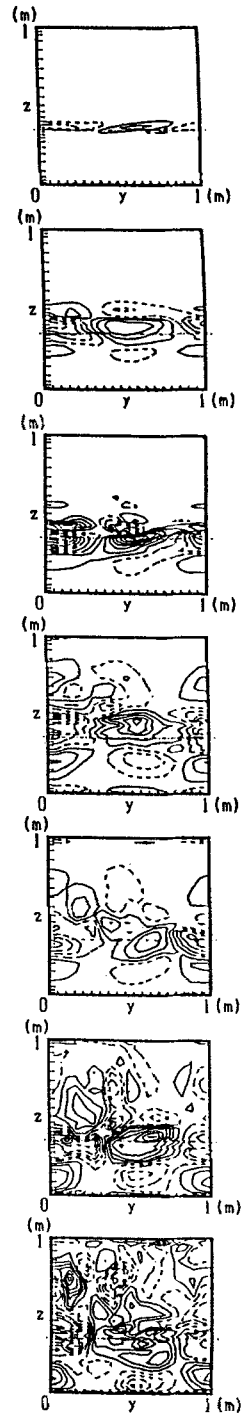

Fig. 5. Streamwise vortices (ξ) in the yz cross-section (x is the position indicated by arrows in Fig. 4) at seven time stages, same as Fig. 3. Contour interval is $0.5\,s^{-1}$.

value of x for the cross-section is indicated by arrows in Figure 4). The streamwise vortices appear as a pair of counter-rotating vortices just like the 'ribs' observed in mixing layers (Hussain, 1986). At $t = 23.8$ s, a large eddy structure overhangs and breaks down (Figures 3e and 4e). In the case of a mixed layer, the life of the organized structure is complete at this time, and it then contributes to a new velocity profile in the mixed layer, i.e., the velocity difference between the two streams is eliminated by the momentum transfer within the eddy structures. However, in the case of the flow within and above the plant canopy, the velocity profiles are the result of a balance of the pressure gradient and the leaf drag so that they can maintain continuously the inflexion point near the top of the canopy. Before long, 'rolls' are generated again near the canopy top and the cycle is repeated, as mentioned above (Figures 3 and 4f, g). However, the velocity fields are a little more disturbed and the organized structures, although they can be recognized, are not as clear as those in the initial cycle that begins from a non-disturbed flow.

Figure 6 is a perspective view of the isosurface of spanwise vortices at time $t =$ 16.7 s. The existence of 'roll' and 'rib' structures can be clearly seen.

Figure 7 shows the instantaneous velocity fields, with the mean velocity at the top of the plant canopy subtracted, at five time stages; these are the same as the images that would result from instantaneous velocity pictures taken with a camera moving with the mean velocity at the top of the plant canopy. The generation of two large eddies (Figure 7b, at $t = 14.3$ s) and their merging (Figure 7c, at $t =$ 16.7 s) is shown clearly, as mentioned above. Eddy structures are advected by the main stream. The advection of a turbulent vortex segment looks like a wave traveling over a plant canopy that induces plant waving, the phenomenon called 'honami'.

In addition, the eddies are elliptical rather than circular in a vertical cross-section, and their major axes are inclined in the upstream direction, which is important from the viewpoint of the mechanism of momentum transfer between the canopy layer and the atmosphere, as mentioned below.

These numerical results suggest the possibility that wave-like fluctuations of plant canopies can be excited by and are in resonance with the periodic generation of the 3D eddy structure that is induced by the inflexion-point instability of vertical wind profiles at the air-plant interface and then advected by the mean velocity.

b. Statistical characteristics of turbulence

Figure 8 shows vertical profiles of the horizontally-averaged turbulent characteristics (Reynolds stress ($\overline{u''w''}$) and turbulent intensities ($\sqrt{u''^2}$, $\sqrt{v''^2}$, $\sqrt{w''^2}$) at the end of the first cycle ($t = 14.3$ s). A double prime ($''$) indicates a deviation from a horizontally-averaged value. The maximum values of both the Reynolds stress and the turbulent intensities occur at a point slightly above the canopy top and decrease with distance upward or downward. These profiles are closely connected with the generation of disturbances (organized structures) at the air-plant interface

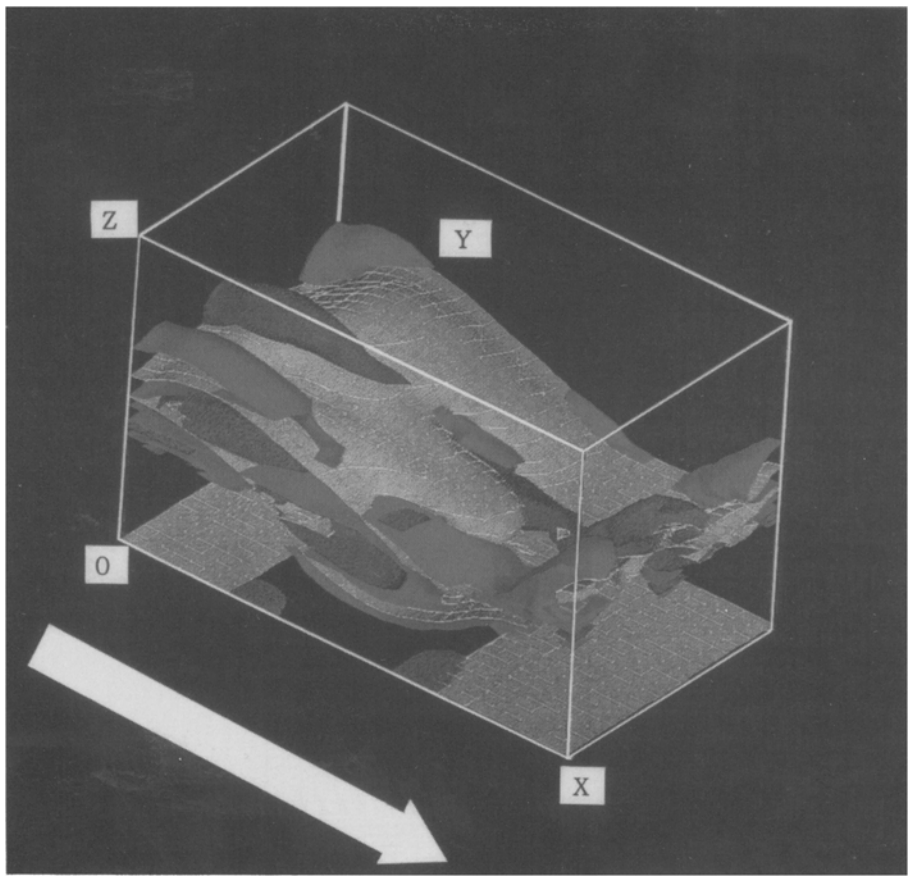

Fig. 6. Perspective view of the isosurface of vortices at time $t = 16.7$ s. Light region: isosurface of spanwise vortices ($\eta = 1.0\,s^{-1}$). Middle region: isosurface of streamwise vortices ($\xi = 1.0\,s^{-1}$). Dense region: isosurface of streamwise vortices ($\xi = -1.0\,s^{-1}$). Flow direction is left to right.

and their diffusion to the upper or lower layers. Figure 9 shows time series of horizontally-averaged turbulent parameters at the top of the plant canopy. The wave-like fluctuations of the Reynolds stress vary in a similar way to the life cycle of the organized structure. The period of this cycle is about 10 s, a value comparable to that observed for short grass (Maitani and Seo, 1984).

c. Relationship between the organized structure and 'sweep' or 'ejection' motion

Figure 10 shows the contour map of the Reynolds stress on three different horizontal planes ($t = 14.3$ s); (1) canopy top, (2) the plane where the horizontally-averaged Reynolds stress has a peak value (designated hereafter as the 'critical height')

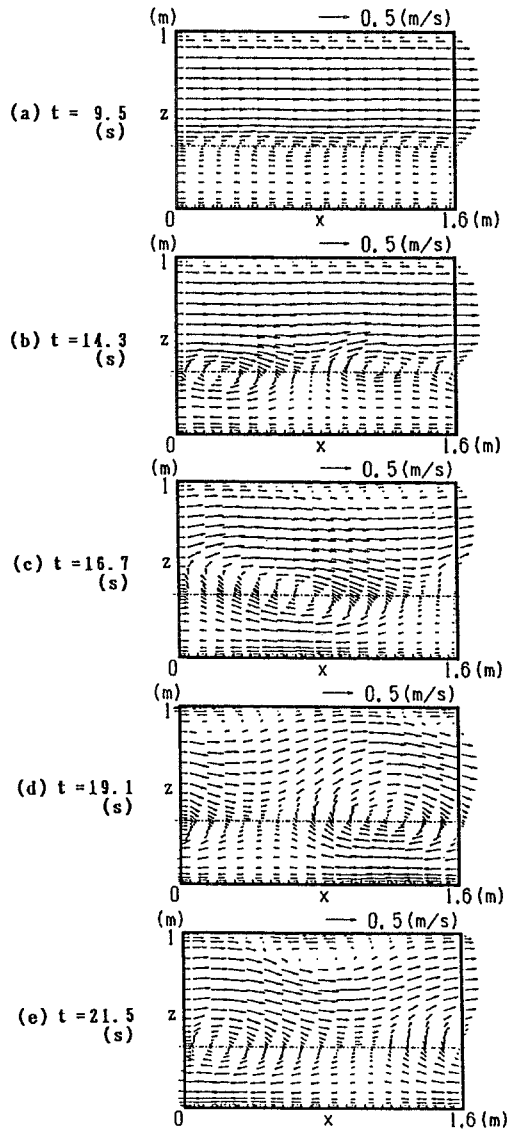

Fig.7. Instantaneous velocity fields in the xz cross-section ($y = 0$), with the mean velocity at the top of the plant canopy subtracted everywhere, at five time stages; (a) 9.5 s, (b) 14.3 s, (c) 16.7 s, (d) 19.1 s, (e) 21.5 s.

and (3) a location above the critical height which is equal to that from the canopy top to the critical height. Figure 11 shows the distribution of four types of $\overline{u''w''}$ obtained by quadrant analysis at three different horizontal planes, as in Figure 10 ($t = 14.3$ s). Just at the top of the plant canopy, a strong sweep motion is seen to occur in a narrow area, and a strong ejection is generated above the critical height.

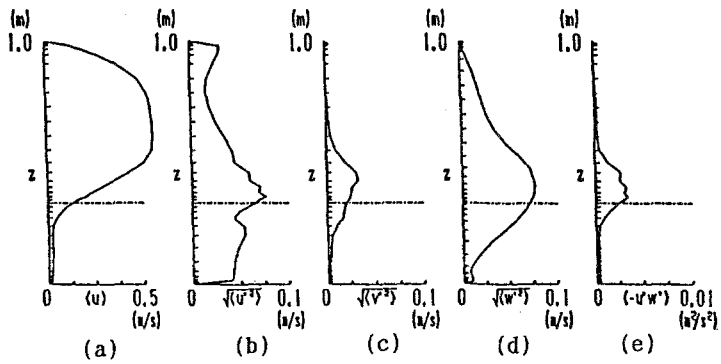

Fig. 8. Vertical profiles of the horizontally-averaged (a) mean velocity, turbulent intensities, ((b) $\sqrt{u''^2}$, (c) $\sqrt{v''^2}$, (d) $\sqrt{w''^2}$) (e) Reynolds stress ($\overline{u''w''}$) at the end of the first cycle ($t = 14.3$ s). Double prime ('') indicates the deviation from the horizontally-averaged value.

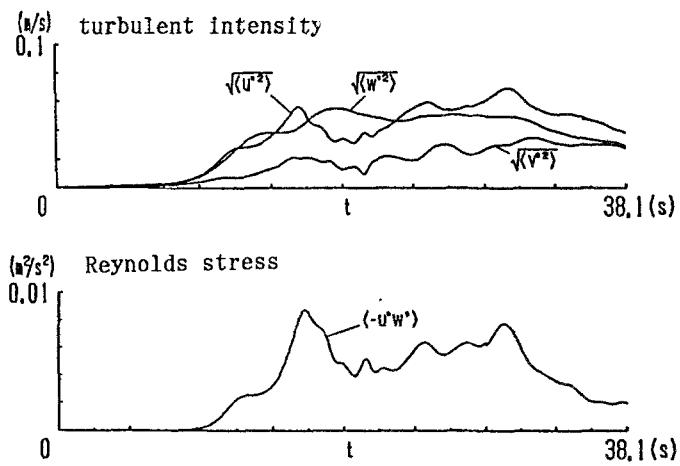

Fig. 9. Time series of horizontally-averaged turbulent parameters at the top of plant canopy. (a) Turbulent intensities and (b) the Reynolds stress.

At the critical height, 'sweep' and 'ejection' have nearly the same strength and width. Figure 12 shows the relative contributions of 'sweep' type fluctuations and those of 'ejection' type to the positive Reynolds stress ($t = 14.3$ s). The sweep motion of turbulence makes the larger contribution to the momentum transport within and just above the plant canopy, whereas the ejection motion prevails in the higher regions. In fact, these tendencies seem to be a common feature of flows within and above plant canopies irrespective of plant species.

Figure 13 shows a vertical cross-section of the instantaneous fluctuating velocity at various heights. These results are similar to those observed in the field observations by Gao *et al.* (1989, Figure 14) and in laboratory flume experiments by

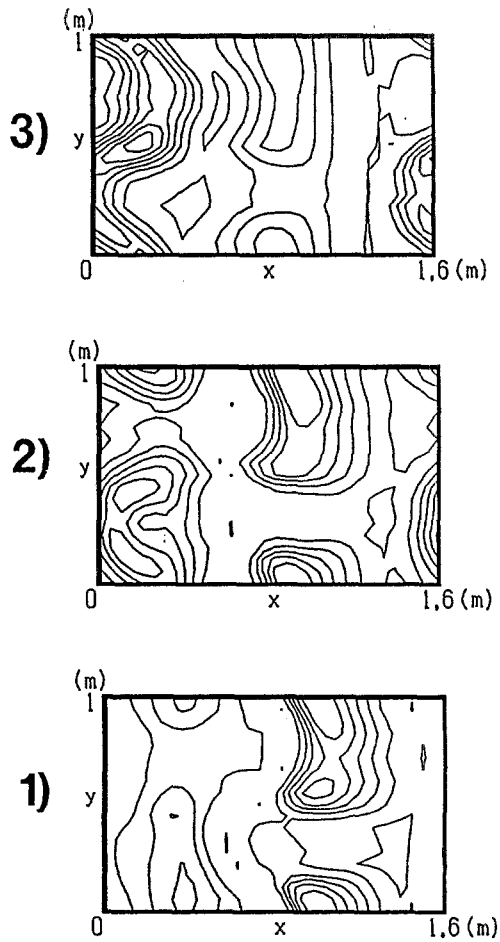

Fig. 10. Contour map of the Reynolds stress at the three different horizontal planes at $t = 14.3$ s; (1) canopy top, (2) the plane where the horizontally-averaged Reynolds stress has a peak value ('critical height') and (3) a location above the critical height that is equal to that from the canopy top to critical height. Contour interval is 0.005 m^2/s^2.

Ikeda and Ota (1992), although there are some differences among these studies in regard to canopy scale and some other details. The major axis of the elliptical eddy in these three studies seems to be inclined to the upstream direction (note the fluctuating velocity vector near the canopy top in Figures 13 and 14), which helps explain the spatial characteristics of sweeps and ejections (Figure 10). Figure 15 is a schematic of the relations of an elliptic eddy and the distribution of sweeps and ejections. Ho and Huerre (1984) suggested in their study of a mixing layer that the inclination of the elliptical eddy, as shown in Figures 13 and 14, generates a positive value of Reynolds stress, whereas a circular eddy does not create a net Reynolds stress. Strictly speaking, this result seems to conflict with the zero lag

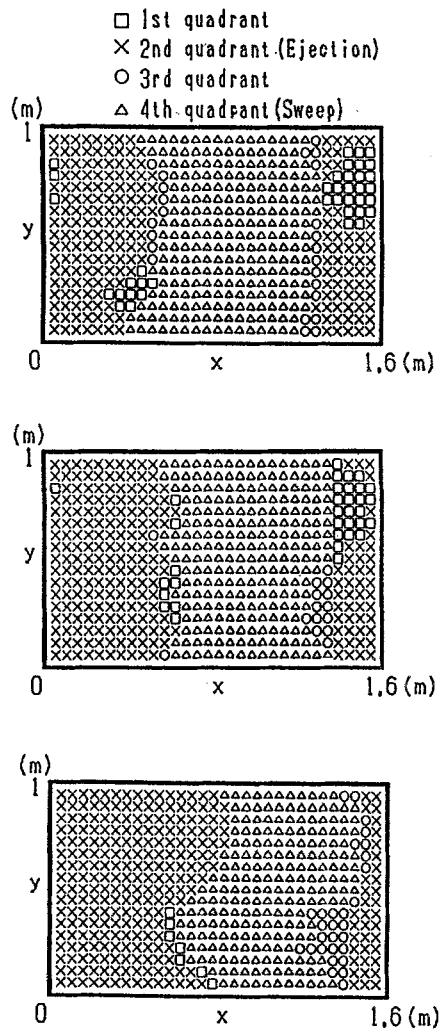

Fig. 11. Distribution of four types of $\overline{u''w''}$ at three different horizontal planes, same as in Fig. 10 at $t = 14.3$ s.; 1st quadrant ($u'' > 0$, $v'' > 0$); 2nd quadrant (identified as ejection, $u'' < 0$, $v'' > 0$); 3rd quadrant ($u'' < 0$, $v'' < 0$) and; 4th quadrant (identified as sweep, $u'' > 0$, $v'' < 0$).

for vertical cross-correlations of vertical velocity observed in the field (Gao *et al.*, 1989). Even if the major axis is a little inclined, there are some possibilities that the significant vertical cross-correlations of vertical velocity can not be observed.

5. Conclusion

This paper has focussed on coherent vortical structures, and has treated them in some detail. In real situations, the canopy top is not homogeneous, and the

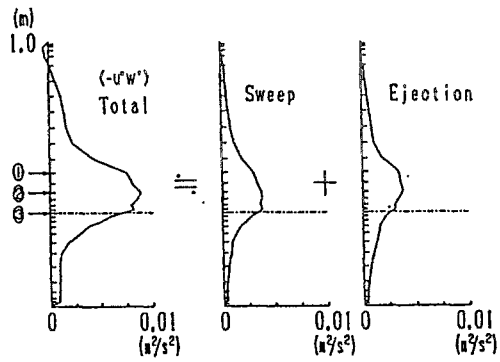

Fig. 12. Ratio of the contribution of 'sweep' type fluctuations and those of the 'ejection' type to the positive Reynolds stress at $t = 14.3$ s.

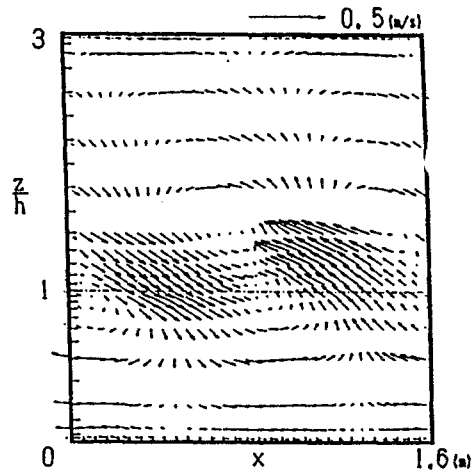

Fig. 13. Numerical result of instantaneous fluctuating velocity in the xz cross-section ($y = 0$, $t = 14.3$ s).

organization of plant canopies is more complicated; hence, various types of organized structures could occur.

The LES model, which simulates air flow within and above the plant canopy layer, has been used to describe the organized structure at the air-plant interface. The following are the main results:

(1) The organized structure of turbulence within and above a plant canopy is characterized by 'rolls' (spanwise vortices) and 'ribs' (streamwise vortices), which are similar to those observed in turbulent mixing layers. The structure has a life cycle.

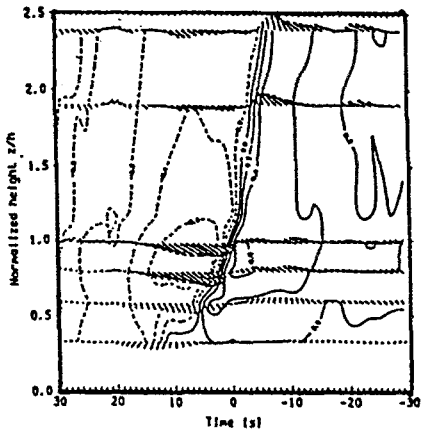

Fig. 14. Ensemble-averaged image of velocity field in the xz cross-section obtained from field observations by Gao *et al.* (1989).

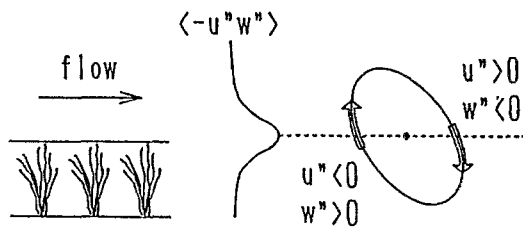

Fig. 15. Schematic of the relations of an elliptic eddy and the distribution of sweeps and ejections.

(2) The advected structure looks like a traveling wave (Honami) and, in fact, wave-like fluctuations of Reynolds stress are produced.
(3) The vertical profiles of Reynolds stress and turbulence intensity obtained by numerical simulation are similar to those observed in field experiments. The results can be explained on the basis of the organized structure of inclined elliptical vortices.
(4) Large eddy structures simulated here agree with observations using quadrant analysis that, within and just above the plant canopy, sweep rather than ejection motion contribute to the momentum transport, while the ejection motion dominates at higher elevations.

Acknowledgements

The present study was supported financially by Grant-in-Aid for Developmental Scientific Research (No. 03452207) from the Ministry of Education, Science and Culture of Japan. Most of the computation was done using the CRAY X-MP in

the Century Research Center (CRC). Thanks also go to Satoshi Inagaki, a student of Tokyo Institute of Technology, for help in performing the computations and producing the figures.

References

Amiro, B. D. and Davis, P. A.: 1988, 'Statistics of Atmospheric Turbulence within a Natural Black Spruce Forest Canopy', *Boundary-Layer Meteorol.* **44**, 267–283.

Baldocchi, D. D. and Meyers, T. P.: 1988, 'Turbulence Structure in a Deciduous Forest', *Boundary-Layer Meteorol.* **43**, 345–364.

Bergstrom, H. and Högstrom, U.: 1989, 'Turbulent Exchange above a Pine Forest; II Organized Structures', *Boundary-Layer Meteorol.* **49**, 231–263.

Bernal, L. P. and Roshko, A.: 1986, 'Streamwise Vortex Structures in Plane Mixing Layers', *J. Fluid Mech.* **170**, 499–525.

Brown, G. L. and Roshko, A.: 1974, 'On Density Effects and Large Structures in Turbulent Mixing Layers', *J. Fluid Mech.* **64**, 775–816.

Deardorff, J, W: 1970, 'A Numerical Study of Three-Dimensional Turbulent Channel Flow at Large Reynolds Numbers', *J. Fluid Mech.* **14**, 453–480.

Finnigan, J. J.: 1979, 'Turbulence in Waving Wheat. II. Structure of Momentum Transfer', *Boundary-Layer Meteorol.* **16**, 213–236.

Gao, W., Shaw, R. H., and Paw U, K. T.: 1989, 'Observation of Organized Structure in Turbulent Flow Within and Above a Forest Canopy', *Boundary-Layer Meteorol.* **47**, 349–377.

Harlow, F. H. and Welch, J. E.: 1965, 'Numerical Calculation of Time-Dependent Viscous Incompressible Flow of Fluid with Free Surface', *Phys. Fluids* **8**, 2182–2189.

Ho, C. M and Huerre, P.: 1984, 'Perturbed Free Shear Layers', *Ann. Rev. Fluid Mech.* **16**, 365–420.

Hino, M., Kanda, M., and Inagaki, S.: 1992, 'Numerical Experiment on the Momentum Transfer at the Air-Plant Interface', *Proc. of Hydraulic Eng., JSCE.* **26**, 689–692. (in Japanese).

Hussain, A. K. M. Falze: 1986, 'Coherent Structures and Turbulence', *J. Fluid Mech*, **173**, 303–356.

Ikeda, S. and Ota, K., and Hasegawa, H.: 1992 'Periodic Vortices at the Boundary of Vegetated Area Along River Bank, *Proc. of Japan Soc. of Civil. Eng.* **443**, 47–54 (in Japanese).

Ikeda, S. and Ota, K.: 1992 'Generation of Honami over Flexible Vegetation', *Proc. Symp. of Turbulent Flow, Japan* **24**, 245–252 (in Japanese).

Inoue, E.: 1955, 'Studies of the Phenomena of Waving Plants (Honami) Caused by Wind. Part 1. Mechanism and Characteristics of Waving Plants Phenomena', *J. Agric. Meteorol. (Japan)* **11**, 18–22.

Inoue, K.: 1981, 'A Model Study of Microstructure of Wind and Turbulence of Plant Canopy Flow', *Bull. Natl. Inst. Agric. Sci.* **A27**, 69–89.

Kawamura, T. and Kuwahara, K.: 1984, 'Computation of High Reynolds Number Flow Around a Circular Cylinder with Surface Roughness', AIAA paper, 84–340.

Kanda, M., Hino, M., and Inagaki, S.: 1992a 'Application of LES Model to the Turbulent Flow Within and Above Plant Canopy', *Proc. Symp. of Numerical Simulation of Turbulence, Japan* **7**, 21–26 (in Japanese).

Kanda, M., Hino, M., and Inagaki, S.: 1992b 'Large Eddy Simulation on Organized Structure Within and Above Plant Canopy', *Proc. Symp. of Turbulent Flow, Japan* **24**, 240–244 (in Japanese).

Kondo. J and Akashi, A.: 1976, 'Numerical Study on the Two Dimensional Flow in Horizontally Homogeneous Canopy Layers, *Boundary-Layer Meteorol.* **10**, 255–272.

Maitani, T. and Seo, T.: 1984, 'Wave-Like Wind Fluctuations Observed in the Stable Surface Layer over a Plant Canopy', *Boundary-Layer Meteorol.* **29**, 273–283.

Maitani, T. and Shaw, R. H.: 1990, 'Joint Probability Analysis of Momentum and Heat Fluxes at a Deciduous Forest', *Boundary-Layer Meteorol.* **52**, 283–300.

Raupach, M. R., Finnigan, J. J., and Brunet, Y.: 1989, 'Coherent Eddies in Vegetation Canopies', *Proc. Fourth Australasian Conf. on Heat and Mass Transfer.* Christchurch, New Zealand, 9–12 May, 75–90.

Raupach, M. R., Antonia, R. A., and Rajagopalan, S.: 1991, 'Rough-Wall Turbulent Boundary Layers', *Appl. Mech. Reviews* **44**, 1–25.

Schumann, U.: 1975, 'Subgrid Scale Model for Finite Difference Simulations of Turbulent Flows in Plane Channels and Annuli', *J. Comp. Phys.* **18**, 376–404.

Shaw, R. H. and Seginer, I.: 1987, 'Calculation of Velocity Skewness in Real and Artificial Plant Canopies', *Boundary-Layer Meteorol.* **39**, 315–332.

Shaw, R. H. and Schumann, U.: 1992. 'Large-Eddy Simulation of Turbulent Flow Above and Within a Forest', *Boundary-Layer Meteorol.* **61**, 47–64.

Shaw, R. H., Tavangar, J., and Ward, D. P.: 1983, 'Structure of the Reynolds Stress in a Canopy Layer', *J. Clim. Appl. Meteorol.* **39**, 315–332.

Smagorinsky, J. S.: 1963, 'General Circulation Experiments with the Primitive Equations', *Mon. Weath. Rev.* **91**, 99.

Wilson, N. R and Shaw, R. H.: 1977, 'A High Order Closure Model for Canopy Flow', *J. Appl. Meteorol.* 1197–1205.

Yamada, T.: 1982, 'A Numerical Model Study of Turbulent Airflow In and Above a Forest Canopy', *J. Meteorol. Soc., Japan* **60**, 439–454.

Yoshizawa, A. and Horiuchi, K.: 1985, 'A Statistically Derived Subgrid Scale Kineteic Energy Model for the Large Eddy Simulation of Turbulent Flows', *J. Phys. Soc. Japan* **54**, 2834–2839.